

# Mechanical, morphological and water intake behavior of Mg-Si integrated carbon hybrid composite for marine deckhouse

Amirthaiah Amala Mithin Minther Singh<sup>a</sup>, Panimayam Arul Franco<sup>b</sup>,  
Joseph Selvi Binoj<sup>c,\*</sup>, Amirthaiah Arul Shemin<sup>d</sup>

<sup>a</sup>Department of Mechanical Engineering, DMI College of Engineering, Chennai - 600123, Tamilnadu, India

<sup>b</sup>Department of Mechanical Engineering, University College of Engineering Nagercoil, Konam - 629004, Tamil Nadu, India

<sup>c</sup>Institute of Mechanical Engineering, Saveetha School of Engineering, Saveetha Institute of Medical and Technical Sciences (SIMATS), Chennai - 602105, Tamilnadu, India

<sup>d</sup>Department of Mechanical Engineering, VINS Christian College of Engineering, Nagercoil - 629807, Tamilnadu, India

(\*Corresponding author: [binojlaxman@gmail.com](mailto:binojlaxman@gmail.com))

Submitted: 7 October 2022; Accepted: 21 November 2023; Available On-line: 3 January 2024

**ABSTRACT:** The automated boat's deckhouse is made of deforested wood and glass fiber, harming producers, fishermen, and marine life. In context, researchers are attempting to make composites from waste and replace synthetic materials with natural composites. In the present work, a Carbon/Mg/Si/polyester hybrid composite is developed as a potential replacement for wood in marine deckhouse construction. Impact, tensile, flexural, Rockwell and Brinell hardness were tested using ASTM standards, as well as weight absorption in fresh and seawater. Scanning electron microscopy (SEM), microanalysis (EDAX), Fourier-transform infrared spectroscopy (FTIR) and Raman Spectroscopy techniques were used to identify microstructure, elements, and functional groups. Thermogravimetric analysis and differential scanning calorimetry (DSC) are used to determine the thermal stability and heat intake/rejection of the hybrid composite. Novel hybrid composites with Mg-Si fillers improve the mechanical strength, adhesion, corrosion resistance, and deckhouse life span in marine environments.

**KEYWORDS:** Discarded ceramic carbon powder; Hybrid composites; Marine deckhouse; Mechanical behavior; Mg-Si

**Citation/Citar como:** Singh, A.A.M.M.; Arul Franco, P.; Binoj, J.S.; Arul Shemin, A. (2023). "Mechanical, morphological and water intake behavior of Mg-Si integrated carbon hybrid composite for marine deckhouse". *Rev. Metal.* 59(3): e246. <https://doi.org/10.3989/revmetalm.246>

**RESUMEN:** *Comportamiento mecánico, morfológico y de absorción de agua del material compuesto híbrido de carbono integrado Mg-Si para casetas marinas.* La caseta de cubierta de los barcos automatizados está hecha de madera deforestada y fibra de vidrio, lo que perjudica a los productores, los pescadores y la vida marina. En este

**Copyright:** © 2023 CSIC. This is an open-access article distributed under the terms of the Creative Commons Attribution 4.0 International (CC BY 4.0) License.

contexto, los investigadores intentan fabricar materiales compuestos a partir de residuos y sustituir los materiales sintéticos por materiales compuestos naturales. En el presente trabajo, se desarrolla un compuesto híbrido de carbono/Mg/Si/poliéster como posible sustituto de la madera en la construcción de casetas marinas. Se ensayó la resistencia al impacto, a la tracción, flexión, y se midió la dureza Rockwell y Brinell utilizando las normas ASTM, así como la absorción de peso en agua dulce y de mar. Se utilizaron microscopía electrónica de barrido (MEB), microanálisis (EDAX) y espectroscopia FTIR/Raman para identificar la microestructura, los elementos químicos y los grupos funcionales. El análisis termogravimétrico y la calorimetría diferencial de barrido (CDB) se utilizaron para determinar la estabilidad térmica y la absorción/rechazo de calor del material compuesto híbrido. Los nuevos materiales híbridos con refuerzo de Mg-Si mejoran la resistencia mecánica, la adherencia, la resistencia a la corrosión y la vida útil de las casetas en ambientes marinos.

**PALABRAS CLAVE:** Casetas marinas; Comportamiento mecánico; Materiales compuestos híbridos; Mg-Si; Polvo de carbón cerámico desechado

**ORCID ID:** Amirthaiah Amala Mithin Minther Singh (<https://orcid.org/0000-0001-6528-1518>); Panimayam Arul Franco (<https://orcid.org/0000-0002-3464-1127>); Joseph Selvi Binoy (<https://orcid.org/0000-0002-7222-4463>); Amirthaiah Arul Shemin (<https://orcid.org/0009-0000-0725-6859>)

## 1. INTRODUCTION

The mechanized boat's marine deckhouse is made of wood and glass fiber. The wood is obtained by felling trees, and glass fiber is extremely poisonous to marine canoe builders, fishermen and marine species. Metal-ceramics combine to form a particle-strengthened hybrid composite that can be used in a variety of applications. Power, stiffness, fatigue, resilience, crack resistance, thermal stability and other mechanical properties are being imparted. One of the key causes of internal structure formation with excellent stiffness and strength in hybrid composites is interfaces between reinforcing micro particles and metal binders resin (Astafurov *et al.*, 2014). Ceramic composites are very hard, strong, rigid and Silicon Carbide (SiC) ceramics provide significant improvements in thermal and mechanical properties such as hardness, tensile strength and corrosion resistance, making them ideal for a variety of structural applications (Džunda *et al.*, 2019). Carbon (C) is a nonmetal member in group 4A with an atomic number of 6 and an electron configuration of  $1s^2 2s^2 2p^2$ . For other metals that have weak Van der Waals bonds, the presence of atoms in the carbon layer has a strong bonding nature (Güler and Bağcı, 2020).

The Indian coastline stretches about 8118 kilometers. In Tamilnadu and Kerala, about 16.5 million fishermen is working in fish industry, followed by 0.02 million canoes. Tamil Nadu and Kerala have 75-foot-long canoe boats with 13–21 layers of glass fiber and 5–9 layers of woven roving on bottom hull. The canoe's total weight is estimated to be between 40 and 60 tonnes (Chandrika *et al.*, 2013; Singh *et al.*, 2018; Report ICSF, 2023). For a long time, more than two lakhs canoe fishing boats have been used for fishing in the coastal areas of Tamilnadu and Kerala. Composites of Al/Mg<sub>2</sub>Si are very appealing materials for structural applications such as aerospace and automotive. The density and thermal expansion coefficient of Mg<sub>2</sub>Si are both very low at  $1.99103 \text{ kg/m}^3$  and  $7.5 \times 10^{-6} \text{ K}^{-1}$  respectively. With

melting temperatures of  $1085 \text{ }^\circ\text{C}$ , hardness of  $4.5 \times 10^9 \text{ N-m}^2$  and elastic modulus of  $120 \text{ GPa}$ , it has a high melting temperature, hardness and elastic modulus. Segregation of primary Si from Mg<sub>2</sub>Si particles in the reinforcement layer confers superior wear resistance to the casting processes in hybrid composites (Robertson *et al.*, 2009; Zhang *et al.*, 2000; Kumar Gupta *et al.*, 2018).

Monolithic materials cannot achieve the properties of modern applications derived from conventional materials functions in recent scenario. As a result, a modern production method for the fabrication of hybrid composites must be introduced. The key benefit of a hybrid composite is that it combines more than two materials without causing a chemical reaction, giving each material better characteristics than composites. Due to its broad range of excellent properties for a variety of applications, ceramics have been used as a matrix in the manufacturing of many composites (Moya *et al.*, 2008; Rodriguez-Suarez *et al.*, 2007; Smirnov A *et al.*, 2019; Singh *et al.*, 2019a). Ceramic-based composite materials are brittle and are not appropriate for extreme loading applications due to inadequate surface finish and induced cracking, which results in unpredictable part failure. By adding metal reinforcements, these failures can be resolved (Gutierrez-Gonzalez *et al.*, 2008; Wing *et al.*, 2016). The addition of a few ductile second phase materials in the composites will toughen the brittle natured ceramic matrix. These composites also known as cermets are used to enhance the mechanical, thermal, electrical and magnetic properties of ductile and high wear-resistant ceramics. This has the potential to avoid catastrophic failure by reducing the development of crack propagation (Smirnov and Bartolomé, 2012; Wing and Halloran, 2017).

The bonding nature of SiC and MgO between particle and metal matrix is found to be excellent, with higher tensile and yield strength and lower magnitude porosity (Smirnov *et al.*, 2018). Using SEM micrographs, the impact of particles reinforced under the machined surface is observed with negligible craters, indicating that SiC particles with Mg matrix

have better mechanical properties (Jayakumar and Annamalai, 2019; Vijayabhaskar and Rajmohan, 2019; Singh *et al.*, 2019b). The aim of this work is to use novel metal integrated ceramic composites to fabricate the deckhouse of a boat. Wood and glass fiber make up a traditional boat deckhouse, whereas the glass fiber is extremely poisonous to producer, fishermen, marine species and wood is harvested by cutting trees, which results in deforestation. Hence, researchers looked for a better alternative to wood by using hybrid composites to replace deckhouses. However, because of seawater, the wood deckhouse decomposes after a few years.

In this study, carbon with Mg and Si as filler materials hybrid composites is used to replace wood in the construction of deckhouses. One of them is ceramic carbon powder (i.e coconut shell), which is discarded in large quantities every year. Using the hand layup process, ceramic carbon powder microparticles, as well as Mg and Si fillers, were mixed with polyester resin to form hybrid composites. The incorporation of metals Mg and Si into ceramic carbon hybrid composites improves mechanical strength, adhesion, corrosion resistance and life span of deckhouses that are exposed to the marine environment.

## 2. MATERIALS AND METHODS

### 2.1. Materials

Carbon micro particles, Magnesium and Silicon microparticles were used in this research work (Fig.

1a and 1b). The carbon micro particle is made from the coconut shell's synthesis. The carbon, magnesium and silicon microparticles are 40  $\mu\text{m}$  in size. Discarded coconut shells (i.e ceramic carbon powder), magnesium, silicon microparticles, polyester resin, cobalt and methyl ethyl ketone peroxide make up the hybrid composite.

### 2.2. Hybrid composite fabrication

One of the basic techniques used to produce composite and hybrid composite is the hand layup technique. By weight or volume fraction process, the resin and hardener are mixed in proper proportions. The hardener is a critical element in the setting and curing action of fabricated composite and it is carefully mixed. The powdered micro particles of carbon (i.e discarded coconut shell) and Mg-Si were combined with the unsaturated polyester resin in the proper proportions to form hybrid composites. The metal-incorporated ceramic micro particles were roughly mixed into the prepared resin. Then, by using the hand layup process the prepared reinforcement and matrix is distributed in the die layer by layer. Carbon serves as the reinforcing element within the composite material and are often organized in a particular configuration (random) to fabricate the hybrid composite material. The fabricated specimens of metal integrated ceramic hybrid composite are shown in Fig. 1c. Several hybrid composites containing a mixture of carbon micro particles and Mg/Si (S1, S2, S3, S4 and S5) were made in proportions of 95 %/5 %, 90 %/10 %, 85 %/15 %, 80 %/20 %,

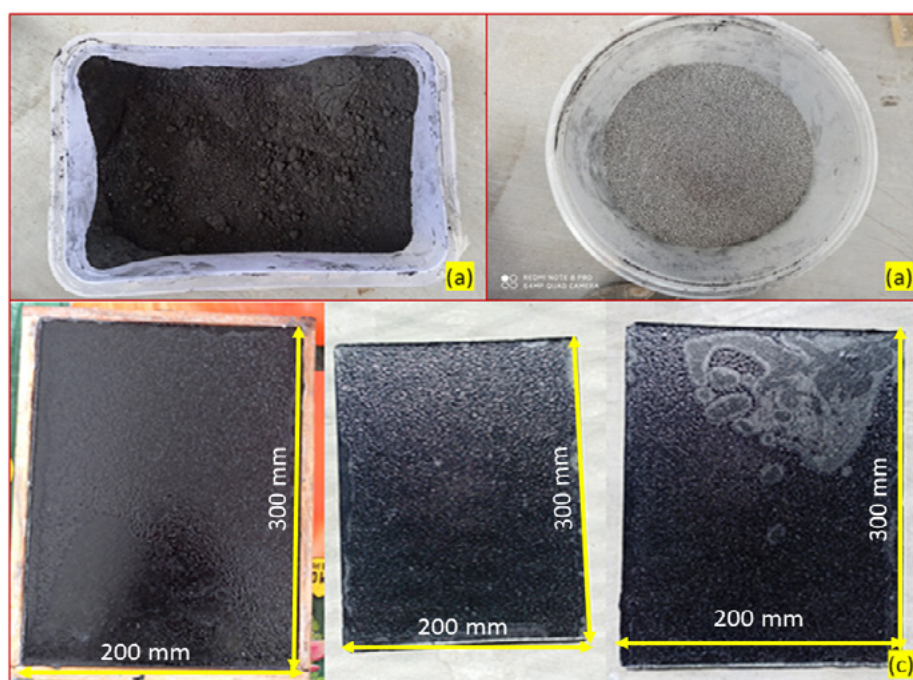


FIGURE 1. a) Carbon microparticle, b) Mg-Si microparticle and c) Fabricated Carbon/Mg-Si Hybrid Composites.

TABLE 1. Hybrid Composite Compositions

| S. No | Specimen Name                        | Carbon Micro Particles (%) | Metal Mg-Si (%) |
|-------|--------------------------------------|----------------------------|-----------------|
| 1     | GF Conventional (Wood & Glass Fiber) | -                          | -               |
| 2     | S1                                   | 95                         | 5               |
| 3     | S2                                   | 90                         | 10              |
| 4     | S3                                   | 85                         | 15              |
| 5     | S4                                   | 80                         | 20              |
| 6     | S5                                   | 75                         | 25              |

75%/25%, respectively. Table 1 shows the fabricated hybrid composite specimens along with the traditional material.

### 3. EXPERIMENTAL ANALYSIS

#### 3.1. Mechanical property studies

The tensile and flexural tests were carried out on a Universal Testing Machine (UTM) in accordance with ASTM D638 and D790 respectively. The Charpy Impact Testing Machine is used to conduct the impact test in accordance with ASTM D256. Three samples of traditional composites (GF), S1, S2, S3, S4 and S5 hybrid composites were tested in this study. The Rockwell and Brinell Hardness Testing Machines were used to evaluate hardness in accordance with ASTM E18 and ASTM E10 using the Eq. (1) and Eq. (2) respectively.

$$\text{Rockwell Hardness Number} = N - \frac{h}{s} \quad (1)$$

where, N denotes the number of specific Rockwell hardness units, h denotes the permanent depth of an indentation in millimeters and s denotes the scale unit (0.001mm for 15N, 30N, 45N, 15T, 30T, 45T). Steel ball indenter scale of 130 units.

$$\text{Brinell Hardness Number} = 0.102 \times \frac{2F}{\pi D(D - \sqrt{D^2 - d^2})} \quad (2)$$

where, F is the test force in N, D is the ball diameter in mm and d is the indentation's mean diameter in mm.

#### 3.2. Weight absorption studies

Weight absorption method is used to determine the rate at which a material's weight is reduced as a result of absorption capacity. This experiment is carried out on fabricated specimens of traditional composites (GF), S1, S2, S3, S4 and S5 hybrid composites. The specimens were submerged in freshwater and seawater for 90 days and their weight is recorded at various intervals. The following Eq. (3) is used to measure the water absorption potential.

Weight Absorption Capacity =

$$\frac{\text{Initial Weight} - \text{Final Weight}}{\text{Initial Weight}} \times 100 \quad (3)$$

#### 3.3. Composite characterization

Scanning electron microscopy (SEM), micro-analysis (EDAX), Fourier-transform infrared spectroscopy (FTIR) and Raman Spectroscopy techniques were used to characterize the fabricated hybrid composites. The SEM, EDAX, FTIR and Raman Spectroscopy experiments were carried out according to ASTM standards ASTM E 1829-97, ASTM E1508-98, ASTM E168 and ASTM E1840 respectively. The mitigation or resolution of potential ageing effects in composite materials, such as Mg-Si integrated carbon hybrid composites, is a crucial factor to ensure their long-term performance and durability. The potential ageing effects encompass the selection of appropriate materials, the application of protective coatings and the execution of environmental testing.

The microstructure of the specimen is inspected using SEM analysis. The surface of the specimen to be examined is coated with gold until it is tested. The scanner's probe will travel over the specimen surface, capturing the image structure at various magnifications. The EDAX device is used in conjunction with the SEM to complete the mission. By moving the probe over the surface, the spectrum is reflected on the monitor. The existence of inorganic compounds, atomic weight and molecular weight are all explained by this spectrum. The FTIR is used to detect the presence of organic compounds in specimens by avoiding infrared rays that would otherwise fall on the surface. Via rotational and low-frequency modes, Raman spectroscopy analyses the presence of molecules in vibrational modes. The Raman scattering light experiment method can be used to measure it. The strength peak, stokes and anti-stokes peaks are used to analyze it.

## 4. RESULTS AND DISCUSSIONS

### 4.1. Mechanical behavior of hybrid composites

#### 4.1.1 Tensile Testing

From Fig. 2 it is observed that specimen S3 has a higher tensile strength than Specimens S1, S2, S4, S5 and conventional composites. The inclusion of 15% metal particles Mg and Si combined together with the 85% of carbon micro particles resulted in higher tensile strength in Specimen S3 hybrid composites owing to better withstanding capacity of load applied and enriches the tensile strength of composite. This S3 specimen with a high tensile strength can be recommended to build the deckhouse of a mechanized boat.

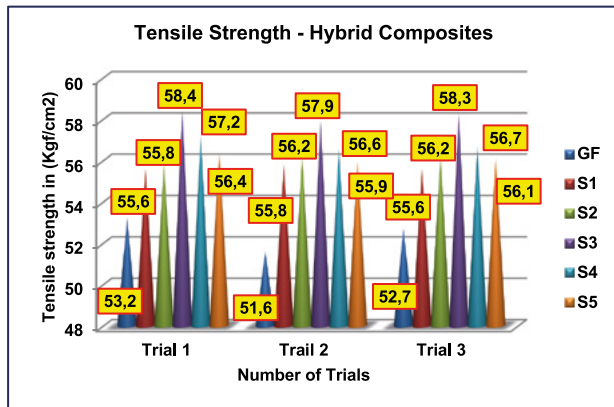


FIGURE 2. Tensile Strength of Fabricated Hybrid Composites.

#### 4.1.2. Flexural Testing

According to Fig. 3 Specimen S3 has a higher flexural strength than Specimens S1, S2, S4, S5 and conventional specimens. The addition of 15% metal particles Mg and Si together with the 85% of carbon micro particles resulted in higher flexural strength in Specimen S3 hybrid composites. The incorporation of Mg and Si in hybrid composite withstander the load applied and enriched the flexural strength of composite.

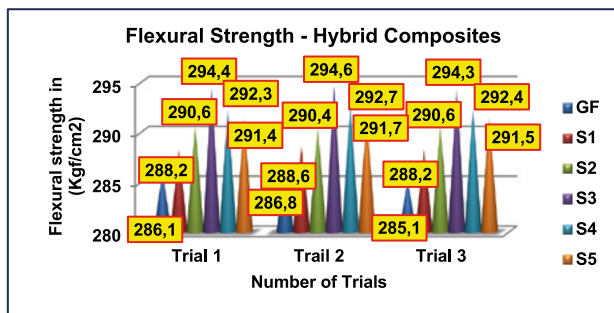


FIGURE 3. Flexural Strength of Fabricated Hybrid Composites.

#### 4.1.3. Impact Testing

The impact values of tested metal integrated ceramic hybrid composites is shown in Fig. 4. It is found that the specimen S3 has a higher impact intensity than other specimens S1, S2, S4, S5 and traditional composites. Similar to tensile and flexural samples, the addition of 15% metal particles Mg and Si as well as 85% of carbon micro particles resulted in higher impact strength in Specimen S3 hybrid composites due to improved load withstanding capacity of the composite.

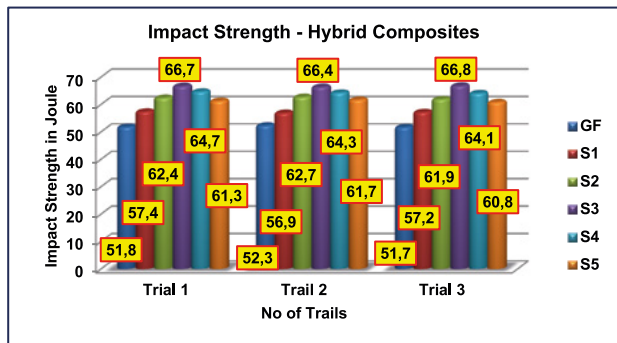


FIGURE 4. Impact Strength of Fabricated Hybrid Composites.

#### 4.1.4. Brinell Hardness of hybrid composites

The fabricated and sized specimen of the metal integrated ceramic hybrid composites subjected to the Brinell load of 2500 kgf is shown in Fig. 5. Specimen S3 has a higher Brinell hardness value than other combinations. The addition of 15% metal particles Mg and Si, as well as 85% of carbon micro particles resulted in a higher Brinell hardness value in Specimen S3 hybrid composites owing to the incorporation of filler particles as well as its withstanding capacity when subject to indentation loads.

149.2HBW (S3 Hybrid Composites) > 133.6HBW (Conventional Specimen)

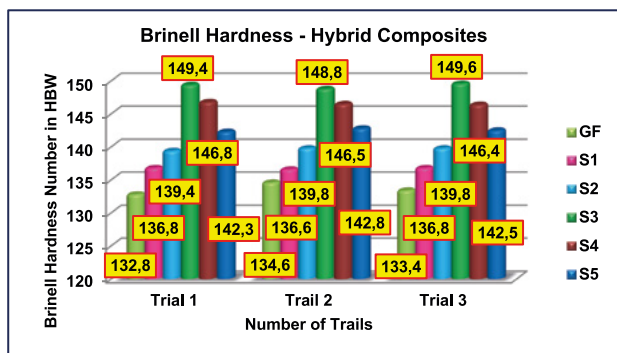


FIGURE 5. Brinell Hardness Number of Fabricated Hybrid Composites.

#### 4.1.5. Rockwell Hardness of hybrid composites

The fabricated and sized specimens of the metal integrated ceramic hybrid composites subjected to 200 kg Rockwell load are shown in Fig. 6. Specimen S3 has a higher Rockwell hardness value than other composite specimens. The addition of 15% metal particles Mg and Si, as well as 85% of carbon micro particles resulted in a higher Rockwell hardness value in Specimen S3 hybrid composites.

93.67 HRB (S3 Hybrid Composites) >82HRB (Conventional Specimen)

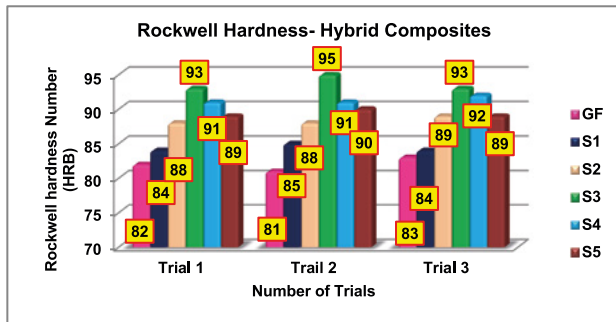


FIGURE 6. Rockwell Hardness Number of Fabricated Hybrid Composites.

The S3 Hybrid composites (85% Carbon + 15% Mg & Si) specimen has far more strength than the other hybrid composite specimens due to the addition of Mg and Si is used as a filler material. By adding small amount of filler materials and its incorporation in carbon-based hybrid composites with proper proportion enhances the mechanical behaviour, as obtained from the various experimental performance. Thus, we can recommend using this S2 Hybrid composites (85% Carbon + 15% Mg & Si) specimen to fabricate the marine

deck house. The performance of Mg-Si integrated carbon hybrid composites in challenging environmental circumstances, such as storms, high humidity or prolonged sun exposure is contingent upon the precise composition of the composite, the manufacturing methodology employed and the intended purpose of material. The composite composition, ambient circumstances, maintenance practices and marine deck house type can affect the durability and longevity of such materials. From the experimental data, the mechanical properties enhanced due to the incorporation of Mg-Si in the carbon hybrid composites.

#### 4.2. Water absorption behavior of hybrid composites

##### 4.2.1. Sea Water medium

The effects of water absorption of fabricated hybrid composite specimens submerged in seawater are shown in Fig. 7a. Water intake behavior affects marine deckhouse composite structural integrity and durability in a complex way. Marine applications like deckhouses use composite materials for lightweight, corrosion-resistant and long-lasting solutions. The water-absorbing characteristics of composite materials, such as Mg-Si integrated carbon hybrid composites, under prolonged exposure to saltwater can be influenced by several factors, including the exact composition of composite and the manufacturing technique employed. In maritime applications, composites are typically engineered to exhibit a high level of resistance to water absorption, particularly in the presence of saltwater. As compared to other hybrid composites, the S3 Hybrid composites (85% Carbon + 15% Mg & Si) specimen consumed less seawater leading to the less intake of water into the specimen owing to the hydrophobic nature of composite.

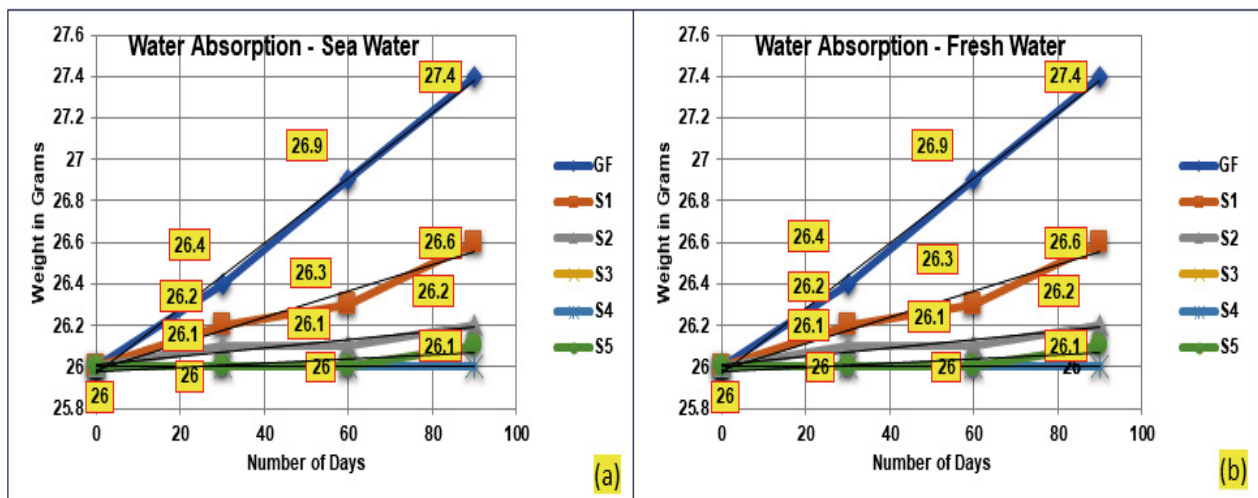


FIGURE 7. Water Absorption of Fabricated Hybrid Composites a) Sea water & b) Fresh water

#### 4.2.2. Fresh Water medium

The effects of water absorption of fabricated hybrid composite specimens submerged in freshwater are as shown in Fig. 7b. As compared to other hybrid composites, the S3 Hybrid composites (85% Carbon + 15% Mg & Si) specimen consumed less freshwater due to the restriction of water flow into the composite as the rough surface of the composite is already filled with the matrix and reinforcement constituents promoting a better hydrophobic nature on the developed hybrid composite.

Scientific study comparing materials for use in marine environments typically takes into account characteristics including how much they weigh, how strong they are, how long they last and how much they cost. Because of their potential benefits in terms of weight reduction, high strength-to-weight ratio and corrosion resistance, advanced composite materials like magnesium-silicon (Mg-Si) and carbon fibers are commonly used from the investigation.

#### 4.3. Specimen characterizations of hybrid composites

##### 4.3.1. Microstructural analysis

Under different magnifications (50000x & 1, 3, 4 & 5 m), the surface microstructure of fabricated hybrid composites S3 (85% Carbon + 15% Mg & Si) is identified using a scanning electron microscope. Fig. 8 shows the morphological structure of S3 hybrid composites at different scales. Specific morphological adjustments will affect the performance of structure. Failure or reduced load-bearing capacity can result from structural integrity loss. Also, the biological growth can increase drag and reduce moving parts efficiency. Moreover, the surface characteristics can affect the material durability and longevity.

The morphological structure of the S3 (85% Carbon + 15% Mg & Si) hybrid composites in various sizes of 1  $\mu\text{m}$ , 3  $\mu\text{m}$ , 4  $\mu\text{m}$ , and 5  $\mu\text{m}$ . It demonstrates how the metal-infused ceramic composite attaches the reinforcement to the matrix. The inter-laminar bonding of the carbon micro particle and Mg-Si mi-

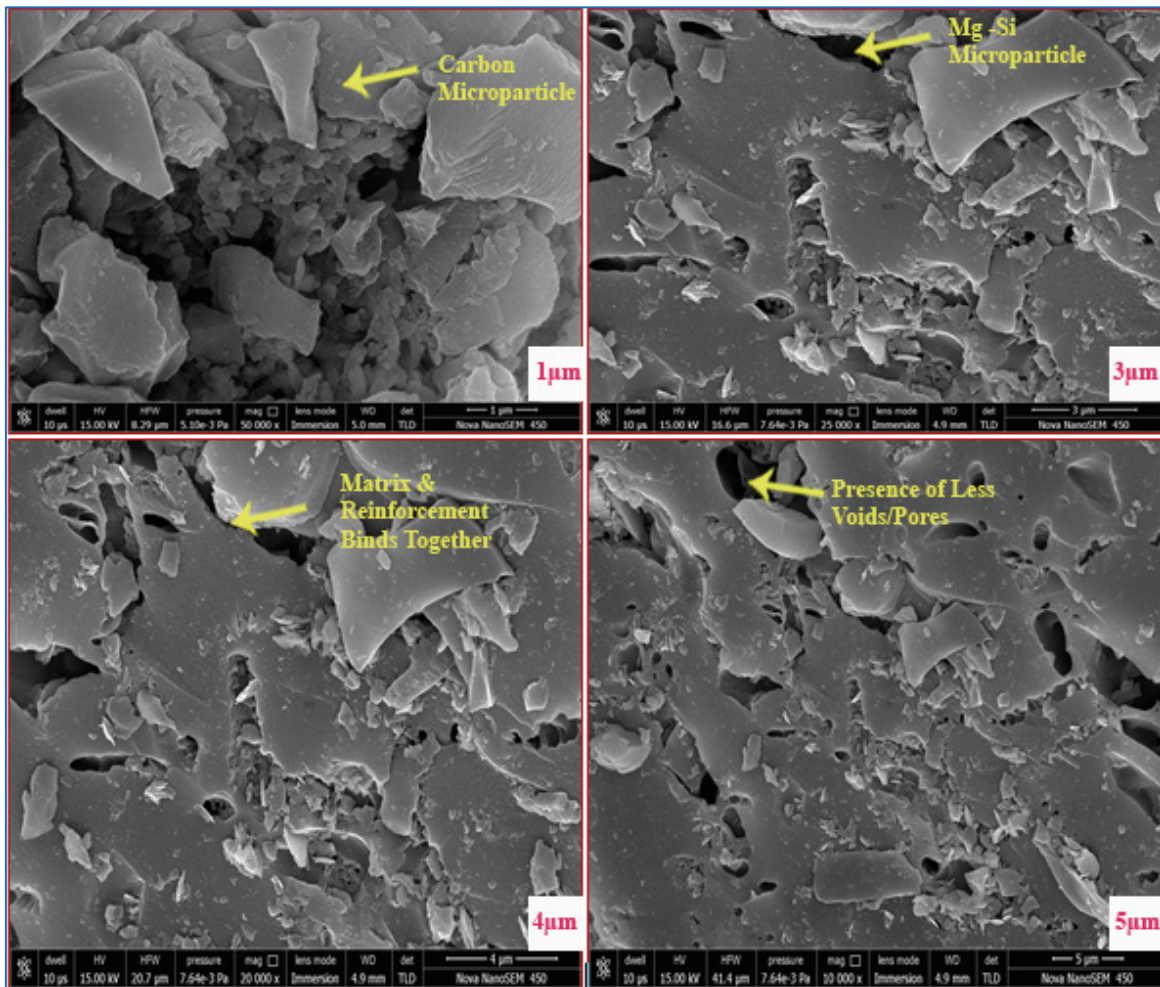


FIGURE 8. SEM Morphology of the S3 Hybrid Composite.

cro particle with the polyester resin is excellent. The existence of pores/voids is discovered to be tiny and insignificant. The matrix adhesion of this metal-ceramic hybrid composite is excellent. The deckhouse of the boat is constructed using carbon and Mg-Si metal hybrid composites.

**4.3.2. Energy Dispersive Atomic Spectroscopy analysis**

The EDAX spectrum of the S3 Hybrid Composite (85% Carbon + 15% Mg & Si) is shown in Fig. 9. The inorganic elements are present in the S3 hybrid composites at peak stage, as shown by the graphical dispersive spectrum. Carbon, Potassium, Oxide, Magnesium, Sodium, Silicon, and Phosphorous are all visible as peaks in the spectrum.

The existence of inorganic elements, as well as their atomic number, molecular weight, and

atomic weight in %age, are shown in Table 2. Carbon 81.49%, Oxide 13.78%, Potassium 2.84%, Phosphorous 0.74%, Sodium 0.66%, Magnesium 0.33%, and Silicon 0.17% are the molecular weight EDAX analysis for S3 (85% Carbon + 15% Mg & Si) hybrid composites. Carbon 87.09%, Oxide 11.05%, Potassium 0.93%, Phosphorous 0.31%, Sodium 0.37%, Magnesium 0.17%, and Silicon 0.08% are the atomic weight EDAX results for S3 (85% Carbon + 15% Mg & Si) hybrid composites.

**4.3.3. Fourier Transforms Infra-Red Spectroscopy analysis**

The FTIR spectrum for S3 hybrid composites (85% Carbon + 15% Mg & Si) is shown in Fig. 10. In the wavelength range of 400–4000 cm<sup>-1</sup>, the FTIR peaks demonstrate the bonding and functional group of organic compounds present in the hybrid composites. The wavenumber corresponding to the bonding and functional group of S3 Hybrid Composite is represented in Table 3.

Six distinct peaks were observed in the S3 hybrid composite FTIR spectrum: 3436.81, 2930.2, 1576.5, 1381.27, 1123.8, and 568.68 cm<sup>-1</sup>. Because of the range excess, the 3436.81 cm<sup>-1</sup> peak has no bonding or functional group. Axisymmetric CH<sub>2</sub> stretching bonding characterizes the 2930.2 cm<sup>-1</sup> peak, which belongs to the Fats, Wax, and Lipids functional group. The N-H plane amide II bonding peak at 1576.5 cm<sup>-1</sup> has a Proteinaceous origin functional group. C-H deformation bonding and a Phenolic & aliphatic Structures functional group characterize the 1381.27 cm<sup>-1</sup> peak. S-O Stretching bonding nature and Sulphates functional group characterize the peak at 1123.8 cm<sup>-1</sup>.

TABLE 2. Chemical Composition of S3 Hybrid Composites using EDAX

| Element | Atomic Number | Molecular Weight (%) | Atomic Weight (%) | Weight (%) |
|---------|---------------|----------------------|-------------------|------------|
| C       | 6             | 81.49                | 87.09             | 15.13      |
| O       | 8             | 13.78                | 11.05             | 3.49       |
| K       | 19            | 2.84                 | 0.93              | 0.17       |
| P       | 15            | 0.74                 | 0.31              | 0.09       |
| Na      | 11            | 0.66                 | 0.37              | 0.10       |
| Mg      | 12            | 0.33                 | 0.17              | 0.07       |
| Si      | 14            | 0.17                 | 0.08              | 0.05       |
| Total   |               | 100.00               | 100.00            |            |

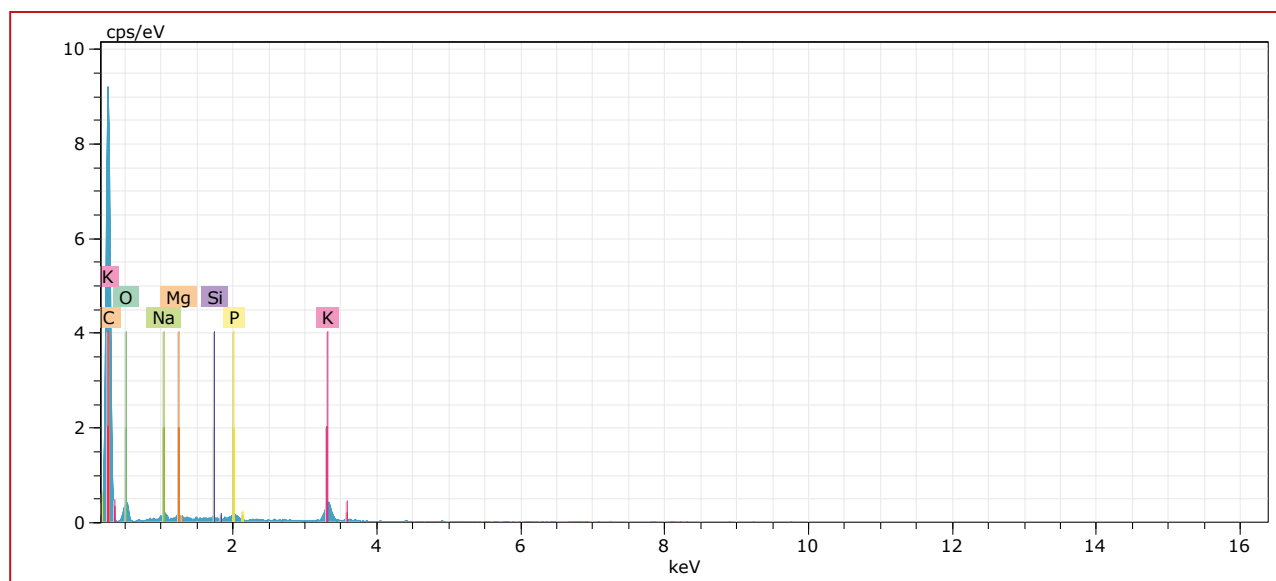


FIGURE 9. EDAX of the S3 Hybrid Composite.

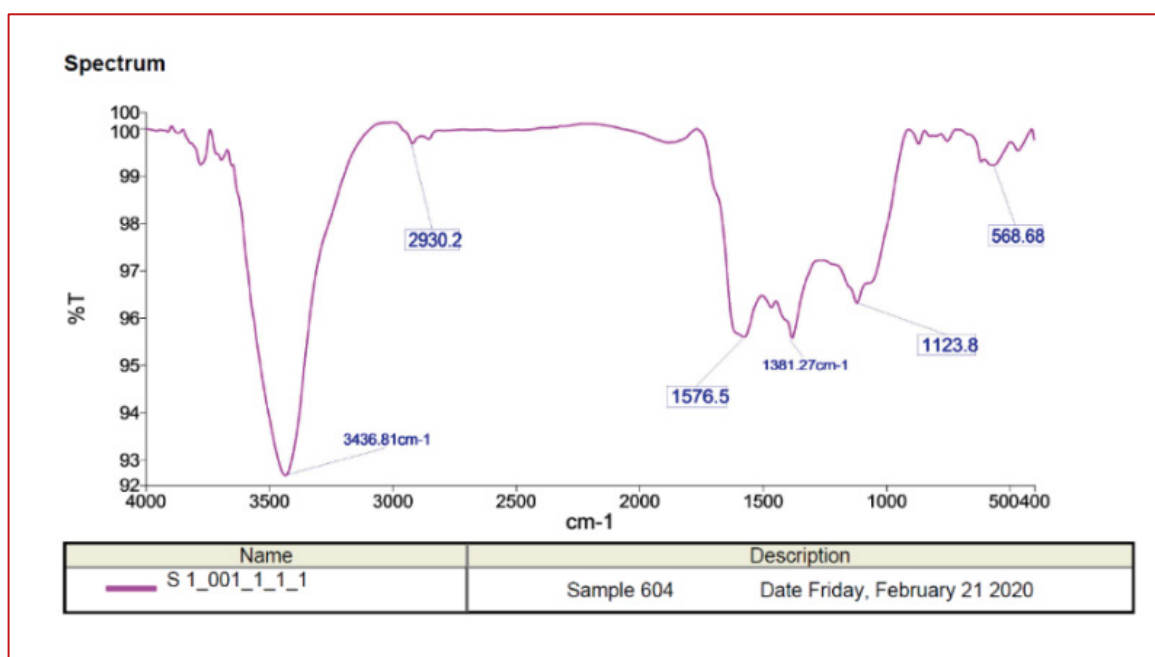


FIGURE 10. Fourier Transform Infra-Red Spectroscopy of the Hybrid Composite.

TABLE 3. FTIR spectrum details of S3 hybrid composite

| Sl. No. | Wavenumber (cm <sup>-1</sup> ) | Bonding                                 | Functional Group                |
|---------|--------------------------------|---|---------------------------------|
| 1       | 3436.81                        | -                                       | -                               |
| 2       | 2930.2                         | Axisymmetric CH <sub>2</sub> stretching | Fats, Wax, Lipids               |
| 3       | 1576.5                         | N-H plane amide II                      | Proteinaceous origin            |
| 4       | 1381.27                        | C-H deformation                         | Phenolic & aliphatic Structures |
| 5       | 1123.8                         | S-O Stretching                          | Sulfates                        |
| 6       | 568.68                         | S-O Bending                             | Gypsum                          |

S-O Bending bonding and the Gypsum functional group characterize the 568.68 cm<sup>-1</sup> peak. It shows that the organic compounds in the S3 hybrid composite have a heavy bonding nature. As a result, S3 hybrid composite can be used to build the boat's deckhouse.

#### 4.3.4. Raman Spectroscopy analysis

Raman spectroscopy determines the vibrational modes of a molecule using rotational and low-frequency modes. The Raman spectroscopy technique is used to obtain the spectrum of S3 (85% Carbon + 15% Mg & Si) hybrid composite (Fig. 11). The spectrum of the S2 hybrid composite revealed two peaks. 1220 cm<sup>-1</sup> and 1610 cm<sup>-1</sup>

are the peak values. The Stokes peak is 1220 cm<sup>-1</sup>, while the intensity peak is 1610 cm<sup>-1</sup>. There is no anti-Stokes peak. The applied nodular frequency is at a low level. With the presence of necessary molecules in the S3 hybrid composites, the presence of an intensity peak indicates better characterization behaviour of the sample.

#### 4.4. Thermal behavior of hybrid composites

Thermogravimetry and a Differential Scanning Calorimeter were used to conduct the thermal analysis. The assay used is a 10 mg hybrid composite of S3 (85% Carbon + 15% Mg & Si

The Differential Scanning Calorimeter curve for the S3 Hybrid Composite is shown in Fig. 12. It shows that an endothermic peak is found at 29.950C with a heat flow rate of -16.88 W/g and a heat flow rate of 793.7 W/g up to 7930C with a heat flow rate of 793.7 W/g. The DSC curve obtained above indicates that it can withstand a temperature of 793.70C. Despite the fact that the sea atmosphere does not hit that high a temperature, its highest temperature is equal to that of the atmosphere.

Thermo gravimetric curve for the S3 Hybrid Composite is shown in Fig. 13. The curve depicts the weight difference as a result of the applied temperature rise. It shows that at a temperature of 630 °C, only a small amount of weight is lost, which is measured as 1.1%. Though the sea atmosphere does not reach that high a temperature, it does reach its highest temperature, which is the

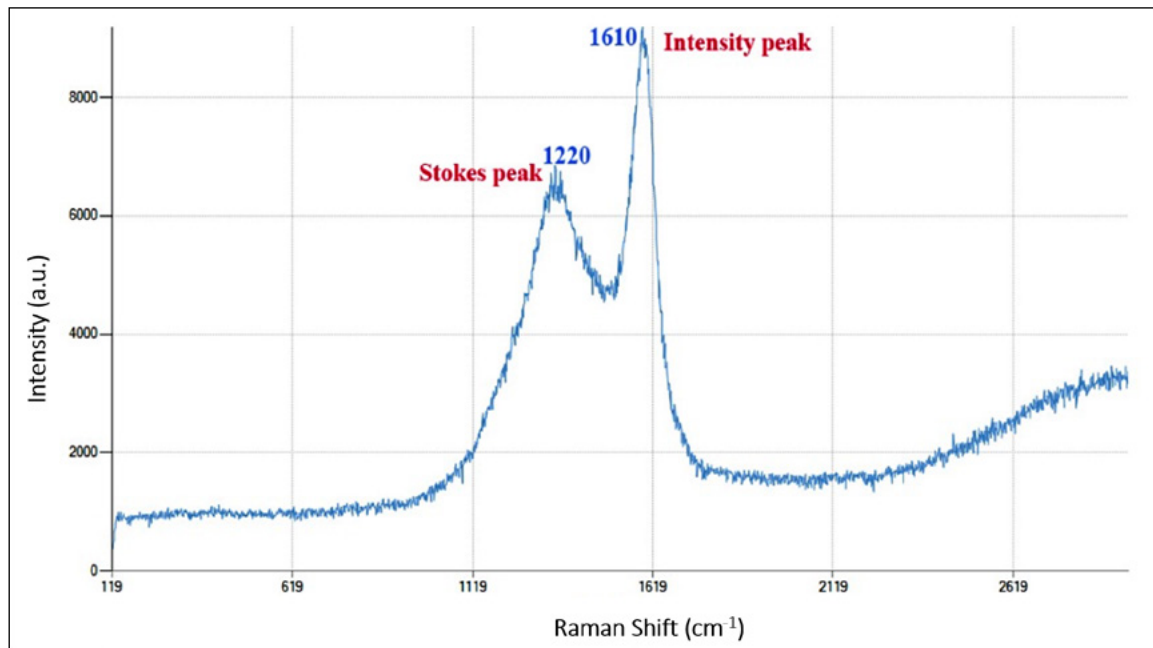


FIGURE 11. Raman Spectroscopy of the Hybrid Composite.

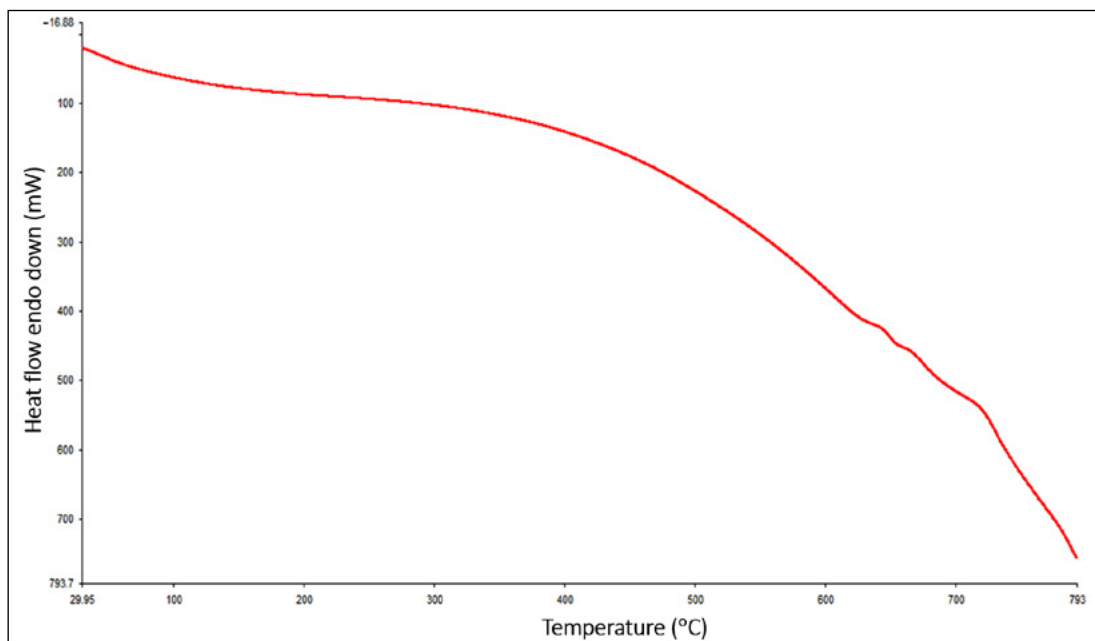


FIGURE 12. DSC of the S3 Hybrid Composite.

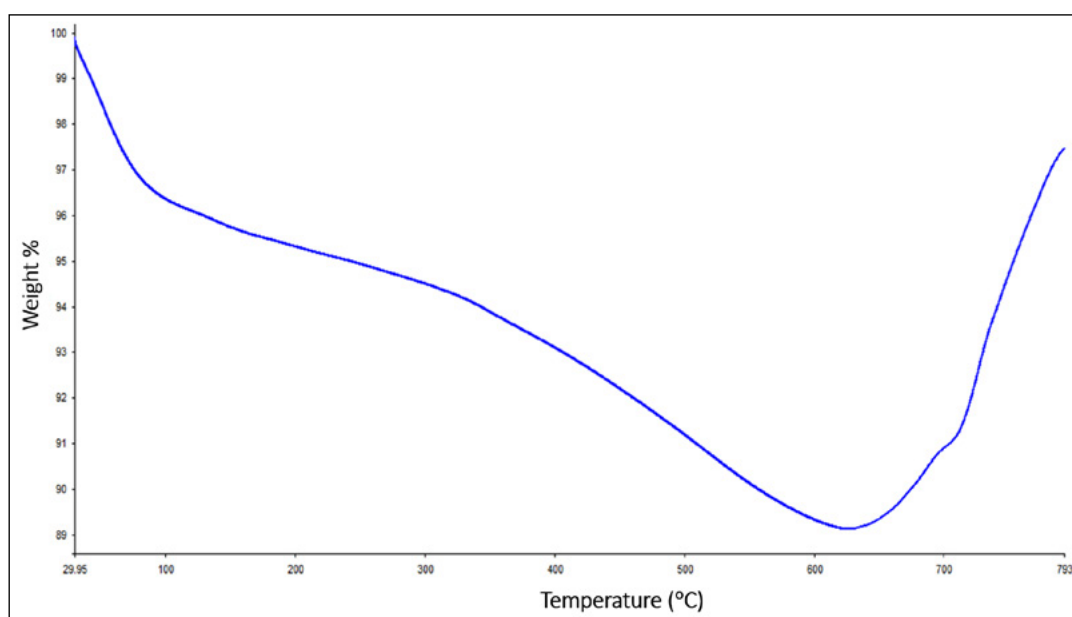


FIGURE 13. TGA of the S3 Hybrid Composite.

temperature of the atmosphere. As a result, the deckhouse of the boat can be constructed using the S3 hybrid composite.

## 5. CONCLUSIONS

- The current project focuses on fabricating the boat's deckhouse using Mg-Si metal combined with carbon micro particles (i.e. discarded coconut shell) reinforced hybrid composites. Based on the investigations it was found that S3 hybrid composite (85% carbon and 15% Mg-Si metal) exposed better tensile, flexural, impact, Brinell and Rockwell hardness than traditional and other fabricated specimens.
- Also, in both fresh and seawater, the water absorption potential of S3 hybrid composite is very low. SEM, EDAX, FTIR, and Raman spectroscopy techniques showed that S3 hybrid composite's microstructure connects metal-incorporated ceramic with unsaturated polyester resin, resulting in excellent adhesion.
- EDAX and FTIR analysis revealed that the existence of inorganic and organic compounds is adequate. The presence of molecules in low-frequency modes was determined by the strength of Raman Spectroscopy peaks.
- The thermal behaviour of the S3 hybrid composite, as measured by TGA and DSC demonstrates that it can withstand the requisite temperature for its weight and heat flow in terms of temperature. The findings revealed that fabricated novel S3 hybrid composites with Mg/Si as filler materials can be used to manufacture marine deckhouses.

## FUNDING

No funding was provided for this study.

## CONFLICT OF INTEREST

The authors declare that they have no conflict of interest.

## DATA AVAILABILITY STATEMENT

Data sharing not applicable to this article as no datasets were generated or analyzed during the current study.

## REFERENCES

- Astafurov, S.V., Shilko, E.V., Ovcharenko, V.E., Dimaki, A.V., Psakhie, S.G. (2014). Development of a structural and rheological model for investigation of peculiarities of deformation and fracture of metal-ceramic composites with multimodal internal structure. *Procedia Mater. Sci.* 3, 568-573. <https://doi.org/10.1016/j.mspro.2014.06.094>.
- Chandrika, S. (2013). *Sea safety programs for artisanal and small-scale fishing communities: the role of gender*. Sea Safety of Small-scale Fishers. International Collective in Support of Fishworkers (ICSF). [https://bobpigo.org/html\\_site/bbn/sep\\_06/pages37-39.pdf](https://bobpigo.org/html_site/bbn/sep_06/pages37-39.pdf).
- Džunda, R., Fides, M., Hnatko, M., Hvizdoš, P., Múdra, E., Medve, D., Kovalíková, A., Milkovi, O. (2019). Mechanical, physical properties and tribological behavior of silicon carbide composites with addition of carbon nanotubes. *Int. J. Refract. Met. Hard Mater.* 81, 272-280. <https://doi.org/10.1016/j.ijrmhm.2019.03.003>.
- Güler, O., Başı, N. (2020). A review on mechanical properties of graphene reinforced metal matrix composites. *J. Mater. Res. Technol.* 9 (3), 6808-6833. <https://doi.org/10.1016/j.jmrt.2020.01.077>.
- Gutiérrez-González, C.F., Bartolomé, J.F. (2008). Damage tolerance and R-curve behavior of Al<sub>2</sub>O<sub>3</sub>-ZrO<sub>2</sub>-Nb multiphase

- composites with synergistic toughening. *J. Mater. Res.* 23 570–578. <https://doi.org/10.1557/JMR.2008.0075>.
- Jayakumar, T., Annamalai, K. (2019). Investigation of Hot Tensile Behavior of Silicon Carbide and Magnesium Oxide Reinforced Aluminum Matrix Composites. *Silicon* 11, 935–945. <https://doi.org/10.1007/s12633-018-9965-2>.
- Kumar Gupta, P., Srivastava, R.K. (2018). Fabrication of Ceramic Reinforcement Aluminium and Its Alloys Metal Matrix Composite Materials: A Review. *Mater. Today: Proc.* 5 (9), 18761–18775. <https://doi.org/10.1016/j.matpr.2018.06.223>.
- Moya, J.S., Díaz, M., Gutierrez-Gonzalez, C.F., Díaz, L.A., Torrecillas, R., Bartolomé, J.F., (2008). Mullite-refractory metal (Mo, Nb) composites. *J. Eur. Ceram. Soc.* 28 (2), 479–491. <https://doi.org/10.1016/j.jeurceramsoc.2007.03.020>.
- Report ICSF (2003). Annual Report 2002-03, South Indian Federation of Fishermen Societies, <https://www.icsf.net/wp-content/uploads/2021/09/Annual-reports-2002-2003-to-2005-2006.pdf>
- Robertson, D.M.V., Sheno, R.A., Boyd, S.W., Austen, S. (2009). A plausible method for fatigue life prediction of boats in a data-scarce environment. ICCM17: 17th International Conference on Composite Materials, Edinburgh, United Kingdom.
- Rodriguez-Suarez, T., Lopez-Esteban, S., Bartolomé, J.F., Moya, J.S. (2007). Mechanical properties of alumina-rich magnesium aluminate spinel/tungsten composites. *J. Eur. Ceram. Soc.* 27 (11), 3339–3344. <https://doi.org/10.1016/j.jeurceramsoc.2007.02.192>.
- Singh, A.A.M.M., Raj, F.M., Arul Franco, P., Binoj, J.S. (2018). Evaluation of mechanical behavior of multifilament discarded fishnet/glass fiber and polyester composites for marine applications. *Mar. Struct.* 58, 361–366. <https://doi.org/10.1016/j.marstruc.2017.11.013>.
- Singh, A.A.M.M., Arul Franco, P., Binoj, J.S., Sahaya Elsi, S., Kumar, M.D. (2019a). Evaluation of Corrosion Resistance and Characterization of Ni-Cr Coated Structure Using Plasma Spray Coating for Marine Hulls. *Plasmonics* 14 (3), 595–610. <https://doi.org/10.1007/s11468-018-0838-8>.
- Singh A.A.M.M., Arul Franco, P., Binoj, J.S. (2019b). Enhancement of corrosion resistance on plasma spray coated mild steel substrate exposed to marine environment. *Mater. Today: Proc.* 15 (Part 1), 84–89. <https://doi.org/10.1016/j.matpr.2019.05.028>.
- Smirnov, A., Bartolomé, J.F. (2012). Mechanical properties and fatigue life of ZrO<sub>2</sub>-Ta composites prepared by hot pressing. *J. Eur. Ceram. Soc.* 32 (15), 3899–3904. <https://doi.org/10.1016/j.jeurceramsoc.2012.06.017>.
- Smirnov, A., Peretyagin, P., Bartolomé, J.F. (2018). Wire electrical discharge machining of 3Y-TZP/Ta ceramic-metal composites. *J. Alloys Compd.* 739, 62–68. <https://doi.org/10.1016/j.jallcom.2017.12.221>.
- Smirnov, A., Peretyagin, P., Bartolomé, J.F. (2019). Processing and mechanical properties of new hierarchical metal-graphene flakes reinforced ceramic matrix composites. *J. Eur. Ceram. Soc.* 9 (12), 3491–3497. <https://doi.org/10.1016/j.jeurceramsoc.2019.02.044>.
- Vijayabhaskar, S., Rajmohan, T. (2019). Experimental Investigation and Optimization of Machining Parameters in WEDM of Nano-SiC Particles Reinforced Magnesium Matrix Composites. *Silicon* 11, 1701–1716. <https://doi.org/10.1007/s12633-017-9676-0>.
- Wing, B.L., Esmonde-White, F., Halloran, J.W. (2016). Microstress in reaction-bonded SiC from crystallization expansion of silicon. *J. Am. Ceram. Soc.* 99 (11), 3705–3711. <https://doi.org/10.1111/jace.14398>.
- Wing, B.L., Halloran, J.W. (2017). Microstress in the matrix of a melt-infiltrated SiC/SiC ceramic matrix composite. *J. Am. Ceram. Soc.* 100 (11), 5286–5294. <https://doi.org/10.1111/jace.15038>.
- Zhang, J., Fan, Z., Wang, Y., Zhou, B. (2000). Hypereutectic aluminum alloy tubes with a graded distribution of Mg<sub>2</sub>Si particles prepared by centrifugal casting. *Mater. Des.* 21, 149–153. [https://doi.org/10.1016/S0261-3069\(99\)00100-4](https://doi.org/10.1016/S0261-3069(99)00100-4).